Published in final edited form as:
Dev Biol. 2011 August 1; 356(1): 40–50. doi:10.1016/j.ydbio.2011.05.002.

The inductive role of Wnt-β-Catenin signaling in the formation of oral apparatus

Congxing Lin[1], **Alexander V. Fisher**[1], **Yan Yin**[1], **Takamitsu Maruyama**[3], **G. Michael Veith**[1], **Maulik Dhandha**[1], **Genkai J. Huang**[1], **Wei Hsu**[3], and **Liang Ma**[1,2,*]

[1] Division of Dermatology, Department of Medicine, Washington University School of Medicine, 660 S. Euclid Avenue, St. Louis, MO, 63110

[2] Department of Developmental Biology, Washington University School of Medicine, 660 S. Euclid Avenue, St. Louis, MO, 63110

[3] Department of Biomedical Genetics & Oncology, University of Rochester Medical Center, 601 Elmwood Avenue, Rochester, NY 14642 U.S.A

Abstract

Proper patterning and growth of oral structures including teeth, tongue, and palate rely on epithelial-mesenchymal interactions involving coordinated regulation of signal transduction. Understanding molecular mechanisms underpinning oral-facial development will provide novel insights into the etiology of common congenital defects such as cleft palate. In this study, we report that ablating Wnt signaling in the oral epithelium blocks the formation of palatal rugae, which are a set of specialized ectodermal appendages serving as Shh signaling centers during development and niches for sensory cells and possibly neural crest related stem cells in adults. Lack of rugae is also associated with retarded anteroposterior extension of the hard palate and precocious mid-line fusion. These data implicate an obligatory role for canonical Wnt signaling in rugae development. Based on this complex phenotype, we propose that the sequential addition of rugae and its morphogen Shh, is intrinsically coupled to the elongation of the hard palate, and is critical for modulating the growth orientation of palatal shelves. In addition, we observe a unique cleft palate phenotype at the anterior end of the secondary palate, which is likely caused by the severely underdeveloped primary palate in these mutants. Last but not least, we also discover that both Wnt and Shh signalings are essential for tongue development. We provide genetic evidence that disruption of either signaling pathway results in severe microglossia. Altogether, we demonstrate a dynamic role for Wnt-β-Catenin signaling in the development of the oral apparatus.

Keywords

Palate; tongue; Shh; Wnt

*Author for correspondence: Mailing Address: Division of Dermatology, Department of Medicine, Washington University, Campus Box 8123, 660 South Euclid Avenue, St. Louis, MO 63110, Tel: (314) 454-8771, Fax: (314) 454-5626, lima@dom.wustl.edu.

The authors have nothing to declare.

INTRODUCTION

Oral cavity forms through a series of fusion events in-between first branchial arch derivatives including maxillary, mandibular and frontal nasal prominences. A mature oral cavity is enclosed dorsally by the palate and ventrally by the floor of the mouth. Being the most anterior part of the alimentary tract, it is responsible for sensing and the initial mechanical processing of food. In mammals, the oral cavity is separated from the nasal cavity by the complete closure of the secondary palate. This separation is particularly important for swallowing, mastication and speech in humans. The palatal primordia first emerge as bilateral vertical downgrowth from maxillary prominences. As development proceeds, the two palatal shelves (PS) are elevated above the tongue into a horizontal opposition. The continuous expansion towards the midline eventually brings the two PS together which then fuse, and the remaining medial edge epithelium (MEE) is removed through apoptosis and/or epithelial-mesenchymal transition (Gritli-Linde, 2007). The mediolateral growth and midline fusion of palates is of particular interest to developmental biologists and physicians because of high incidence of cleft palates in humans (Gorlin RJ, 2001), whereas the anteroposterior (A–P) development of the secondary palate is much less studied and understood. The secondary palate can be divided into two parts with distinct anatomy: the anterior hard palate which forms the maxillary processes and palatine bone, and the posterior soft palate which is composed of muscle and connective tissues. This regional difference is conferred by differential gene expression during development. Regulatory genes such as *Shox2* (Yu et al., 2005b), *Meox2* (Li and Ding, 2007), *Tbx22* (Liu et al., 2008b), *Msx1* (Zhang et al., 2002), and *Fgf10* (Welsh and O'Brien, 2009) are differentially expressed anteroposteriorly. It's noteworthy that during palatal formation, a set of specialized ectodermal appendages, termed palatal rugae, develop along the A–P axis as transversal ridges on the surface of the hard palate. Early rugae development starts with the induction of epithelial thickening termed placode, and condensation of the underlying mesenchyme. The ensuing morphogenesis includes patterning and vaulting of the mesenchyme towards the oral cavity. Fully developed rugae in adult animals host a variety of sensory cells (Nunzi et al., 2004) as well as cranial neural-crest-related stem cells (Widera et al., 2009). Recently, two groups independently described a unique "posterior interposition"(Pantalacci et al., 2008) in rugae development. They found that coupled with palatal extension, all but one ruga sequentially form at the position just anterior to the most posterior (R1) ruga which forms first and defines the boundary between the anterior and posterior palate. This sequential addition of the rugae also posits a connection to anteroposterior palatal growth and patterning (Pantalacci et al., 2008; Welsh and O'Brien, 2009). Despite these findings, the molecular mechanism regulating rugae formation, as well as how rugae addition contribute to the overall palatal development remains to be elucidated.

The tongue is composed of cranial neural-crest-cell (CNC)-derived fibroblasts, and mesoderm-derived muscles (Hosokawa et al., 2010). The dorsal surface of the tongue is covered by the oral epithelium where taste papillae reside. The early development of the tongue is achieved through epithelial-mesenchymal interactions whereby Shh signaling has been suggested to play a key role (Liu et al., 2004). Nonetheless, the molecular mechanism regulating tongue development is not well understood.

Canonical Wnt signaling is a key player in mediating epithelial-mesenchymal interactions during organogenesis. It is well established that activation of Wnt signaling is the initial step in patterning and specification of ectodermal appendages such as the hair follicle (Andl et al., 2002; DasGupta and Fuchs, 1999; Huelsken et al., 2001), tooth (Liu et al., 2008a), mammary gland (Chu et al., 2004) and taste papillae (Liu et al., 2007). Wnt signaling is also obligatory in regulating organ outgrowth as it is required for limb (Barrow et al., 2003;

Soshnikova et al., 2003) and genital tubercle (Lin et al., 2008) development. The involvement of Wnt signaling in craniofacial development is suggested by a spectrum of phenotypes observed in β-Catenin conditional knock-out (cKO) (Brault et al., 2001) and Tcf/Lef knockout embryos (Brugmann et al., 2007). However, these abnormalities rather reflect a requirement for Wnt responsiveness in CNC-derived mesenchyme but not in the epithelial compartment. In this report, we provide genetic evidence that canonical Wnt signaling in oral epithelium plays a dynamic role in tongue and palate development. Removal of canonical Wnt effector β-Catenin using the *Shh*^{Cregfp} line (Harfe et al., 2004) which confers oral epithelial expression resulted in a complete abolishment of rugae formation, a unique cleft palate at the anterior end of the secondary palate, and microglossia. We show that canonical Wnt signaling is required for rugae induction and subsequent *Shh* induction, which may play a key role in coordinating anteroposterior extension and mediolateral growth of the hard palate. We also demonstrate that the induction of *Shh* expression by Wnt signaling in lingual epithelium is critical for tongue formation.

MATERIALS AND METHODS

Animal maintenance and Tamoxifen treatment

Shh^{CreGFP}, *Shh*^{Creesr}, *RosaR26LacZ*, BATGAL and *Shh*$^{c/c}$ stains were obtained from the Jackson Laboratory (Bar Harbor, MN). *β-Cat*$^{c/c}$ and *β-Cat*$^{ex3/ex3}$ mice are gifts from Dr. Fanxin Long at Washington University in St. Louis. Tamoxifen (Sigma-Aldrich, St. Louis, MO) was given to pregnant female mice by oral gavaging at a dose of 0.2 g/kg body weight.

Histology and immunofluorescence

The procedures for sample preparation and immunofluorescence analysis was previously described (Yin et al., 2006). For Monoclonal β-Catenin antibody (BD biosciences) staining, 1:300 dilution was used. For polyclonal Lef-1 (Cell Signaling) and Myf-5 antibody (Santa Cruz Biotechnology) staining, 1:100 dilution was used.

Scanning Electron Microscopy (SEM)

Samples were fixed in 3% glutaraldehyde and 4% paraformaldehyde (PFA) in PBS (Ph 7.4) for at least 2 days. SEM analysis was then carried out as previously described (Lin et al., 2008).

In situ hybridizations

Whole mount in situ analysis was performed using a standard protocol (Wilkinson, 1992). Briefly, palates were isolated, fixed in 4% PFA and dehydrated through graded methanol solutions. Following that, tissues were pretreated with proteinase K and hybridized with RNA probes at 65 °C for overnight.

For Dig-labeled in situ hybridization and radioactive ^{35}S in situ hybridization, palates and tongues were collected, fixed in 4%PFA, dehydrated through graded ethanol solution, and embedded in paraffin blocks. Following that, 10μm-sections were generated using a microtome. Hybridization were then carried out following a standard protocol (Wawersik and Epstein, 2000). Probes for *Fgf8*, *Shh*, *Ptch1*, *Wnt5a*, *Wnt3*, *Bmp7* and *Lef1* were described previously (Lin et al., 2008). Probes for *Shox2*, *Gli1*, *Wnt10b*, *Wnt10a*, *Wnt9b*, *Axin2*, and *Dkk1* were gifts from Dr. Fanxin Long in Washington University. Probes for *Barx1*, *Meox2*, *Tbx22*, and *β-Catenin* were generated by PCR amplification of specific cDNA fragment of corresponding gene.

β-Galactosidase staining

X-Gal staining was carried out as previously described (Lin et al., 2008).

Skeleton preparation

Embryonic mouse heads were skinned, fixed in 95% ethanol overnight, incubated in acetone overnight, and then stained in a solution containing 0.3% Alcine Blue and 0.3% Alizarin Red.

Statistics

Data were analyzed by unpaired Student's t-test. The number of independent experiments is specified in the Results section.

RESULTS

Activation of canonical Wnt signaling in the palatal rugae

We first examined the expression of Wnt family genes in the mouse palate at embryonic day (E) 14.5. In situ hybridization revealed that both *β-Catenin* and *Lef1* mRNA was highly expressed in all palatal rugae epithelium (arrows in Fig. 1A, E). Consistently, indirect immunofluorescence analysis demonstrated that β-Catenin (arrows in Fig. 1B–D) and LEF1 (arrows in Fig. 1F–H) proteins were more abundant in rugae epithelium, with LEF1 showing clear nuclear localization in rugae placodes. We carefully examined two particular rugae at different developmental stages. The most posterior ruga R1 was the most developed and exhibited clear placode formation (Fig. 1D and H), whereas the ruga anterior to it was just forming and had not shown any epithelial thickening (Fig. 1C and G). Intriguingly, elevated β-Catenin and LEF1 expression can be found in both rugae. Consistently, we observed elevated expression of *Pitx2* and *Tcf1* (arrows in Fig. 1U, W), both modulators and direct downstream targets of Wnt-β-Catenin signaling, in rugae epithelium. Moreover, we also detected *Wnt10a* and *Wnt10b* transcripts in palatal epithelium, with *Wnt10a* having a stronger rugae expression (Supplemental Fig. S1G–H).

To determine whether canonical Wnt signaling pathway is active during rugae formation, we used two well-characterized transgenic mouse lines, BATGAL (Maretto et al., 2003) and Axin2-LacZ (Yu et al., 2005a), to report Wnt activity in developing palatal epithelium. At e14.5, BATGAL expression in anterior rugae was readily discernible by whole mount staining (Fig. 1I), and all rugae cells were stained positive for β-Gal expression (Fig. 1J). On the other hand, expression in posterior rugae was rather weak. Sagittal sections revealed that only a few cells in posterior rugae were positive for β-Gal staining (Fig. 1J′). At e15.5, BATGAL expression could be detected in all rugae (Supplemental Fig. S1D). Axin2-LacZ showed a similar expression in rugae epithelium. Weak β-Gal expression was detected in rugae epithelium as early as e13.5 (Supplemental Fig. S1A), and all rugae can be distinguished by whole mount staining at e15.5 (Supplemental Fig. S1C). All these data indicated activation of Wnt-β-Catenin signaling during rugae development. Notably, we did not detect expression of *Wnt3* and *Wnt9b*, two Wnt genes shown to be associated with cleft palate in humans (Niemann et al., 2004), in palatal epithelium at this stage (Fig. S1E–F).

Wnt-β-Catenin signaling is required for rugae induction

To abolish canonical Wnt signaling in palatal epithelium, we generated palatal epithelial-specific β-Catenin-cKO by crossing the *β-Catenin* conditional knockout allele (Brault et al., 2001) with the Shh^{Cregfp} line which confers Cre activity throughout the palatal epithelium as early as E12.5 (Fig. 1K and L). First, we examined β-Catenin removal in the cKO palates. At E13.5, the deletion of β-Catenin protein was obvious (arrow head in Fig. 1N), but

residual β-Catenin protein can still be detected in the cKO epithelium by immunofluorescence (Fig. 1N, arrow). By E14.5, the cKO palatal epithelium was completely devoid of β-Catenin staining (Fig. 1P). Consistently, rugae-specific *Lef1* mRNA and LEF1 protein, and *Pitx2* mRNA expression was undetectable (Fig. 1R, T, and V). *Tcf1* expression was also downregulated throughout the palatal epithelium (Fig. 1X). These data demonstrated a loss of epithelial Wnt responsiveness in the β-Catenin-cKO. Next, we examined palatal development in these β-Catenin cKOs. No morphological difference in PS was observed in β-Catenin cKOs at E12.5 (Fig. 2A and B). In controls, palatal rugae made their first unequivocal appearance at around E13.5 (Fig. 2C). At E15.5, all rugae were evident by Scanning Electron Microscopy (SEM) (Fig. 2G). On the contrary, mutant palates showed no organized ridge-like structures except a few irregular protrusions at E13.5 (Fig. 2D). From E14.5 onward, mutant palates appeared smooth and showed no sign of rugae formation (Fig. 2F, H and J). This phenotype was confirmed by histological analysis on E17.5 (Fig. 2P). Rugae formation in β-Catenin-cKO was blocked at the initiation stage as DAPI (Fig. 2L) and CD44 staining (Fig. 2N) showed no epithelial thickening and mesenchymal condensations at E14.5, respectively.

In addition to mediating canonical Wnt signaling, β-Catenin also functions to maintain the structure of adherens junctions (AJ) by connecting α-Catenin to E-Cadherin. Thus, we examined expression of AJ proteins by immunofluorescence in β-Catenin-cKOs at E14.5. We found no change in α-Catenin and E-Cadherin expression, and an upregulation of Plakoglobin, which can compensate for β-Catenin in AJs (Supplemental Fig. S2A–F). Moreover, we conditionally removed α-Catenin, the obligatory molecule in AJs from the oral epithelium using the same Shh^{Cregfp} line. Since α-Catenin is indispensable for AJ formation, one would expect this model to have more severe cell-cell adhesion defects than the β-Catenin-cKOs. This is indeed true as the structure of α-Catenin-cKO palatal epithelium was disorganized evidenced by disturbed E-Cadherin expression (Supplemental Fig. S2D′). Nevertheless, rugae formed largely normal in these mutants (Supplemental Fig. S2H). Thus, we reasoned that disturbed cell-cell adhesion is not the underlying mechanism for the complete lack of rugae phenotype in β-Catenin-cKOs.

To test whether β-Catenin is sufficient to induce rugae formation, we used Shh^{cregfp} allele to overexpress a constitutively active β-Catenin allele, $\beta\text{-}Cat^{ex3}$. We showed that instead of inducing rugae formation throughout the palatal epithelium, the ectopic gain of function activation of Wnt signaling disturbed normal rugae patterning. SEM revealed ectopic irregular protrusions and Shh expressing cell-clusters throughout the palatal epithelium (Supplemental Fig. S3). These results suggest that either other genes/signaling pathways are required to cooperate with Wnt-β-Catenin during rugae induction, or additional modulators and/or mechanisms, for example transcriptional regulation of *β-Catenin* mRNA, are required to regulate Wnt activity. It is also possible that the specification of appendage sites is not decided by absolute signaling activity in a particular cluster of cells, but rather by a signal gradient generated between these cells and neighboring cells. Nonetheless, all these data indicate that activation of the Wnt-β-Catenin pathway is critical for the induction of palatal appendages.

Lack of rugae is associated with defective palatal growth

In addition to the lack of rugae, the anteroposterior expansion and mediolateral growth of the mutant palates were also abnormal. At E13.5, the edges of opposing PS appeared parallel to each other in controls (Fig. 2C) whereas in the mutants, the anterior PS were further apart than the posterior (Fig. 2D). From E13.5 to E14.5, we consistently observed that distance between the PSs in β-Catenin cKOs was smaller than controls (n>20 litters examined). Around 30% of mutant palates had already fused at E14.5 whereas all control palates were still separated at this time (Fig. 2C–F, Fig. 3, 4). Meanwhile, A–P expansion of the

secondary palate was slightly shorter in the mutants, which became more obvious at E15.5 (Fig. 2G–H). These findings suggested an overgrowth along the medial-lateral axis at the expense of A–P extension in the β-Catenin-cKOs. The primary and secondary palates eventually met and fused in controls at E15.5 (Fig. 2G, I). In contrast, contact between the two palates never occurred in mutants which left two holes in this region (Fig. 2H, J, arrows). It's noteworthy that incisors and primary palate were severely underdeveloped. Histological analysis on e15.5 palates revealed a well formed primary palate in the control palate (arrow in Fig. 2Q) and an absence of tissue anterior to the secondary palate (asterisk in Fig. 2R) in the mutant. These defects likely contribute to the cleft palate phenotype. However in this study, we focused on analyzing the secondary palate defect.

To further characterize the A–P extension defect of the mutant palates, we examined A–P marker gene expression. Expression of *Shox2*, a hard palate marker, was initiated normally in β-Catenin cKOs at E12.5 (Fig. 3A, B). At E13.5, *Shox2* expressing domain was slanted, demarcating the abnormal shape of the mutant PSs and A–P expansion was slightly reduced (Fig. 3C, D). At E14.5, reduction in A–P expansion of *Shox2* expression domain in the mutant was obvious, and its expression level was also downregulated (Fig. 3E, F). *Barx1* expression domain is complimentary to *Shox2* in both genotypes, suggesting that the initial setup of A–P boundary was normal in β-Catenin cKOs. However, non *Barx1*-expressing anterior palate was smaller in the β-Catenin-cKOs (Fig. 3L, N), consistent with a reduced *Shox2*-expressing domain (compare between the stained region in Fig. 3C–F and unstained region in Fig. 3K–N). On the other hand, posterior *Barx1* expression was comparable between the two genotypes. Furthermore, expression of *Tbx22* and *Meox2*, also posterior markers, was not altered in β-Catenin cKOs (Fig. 3I, J and Supplemental Fig. S4A, B). Next, we performed skeleton staining to examine the formation of palatine bones and maxillary processes, both derivatives of *Shox2*-expressing anterior palate. We found that the overall size of the palatine bone was smaller and A–P expansion of the palatine bone and the maxillary processes was reduced in the mutants (Fig. 3G, H and O). On the other hand, the lower jaw of the mutants is comparable to that of controls (Supplemental Fig. S5). All these data indicated a defective A–P expansion of the *Shox2*-expressing hard palate (indicated by double-headed arrows in Fig. 3C–F, I–N). The imbalanced development of anterior and posterior palates might result from incomplete deletion of β-Catenin in the palatal epithelium at E13.5. To test this possibility, we carefully examined the expression of residual β-Catenin in E13.5 cKO embryos (n>6). We found that residual β-Catenin proteins were not localized to any particular region but rather randomly distributed in the ventral palatal epithelium (Supplemental Fig. S6). Thus, we concluded that this phenotype does not reflect an uneven deletion of the β-Catenin protein. To further explore the cellular mechanisms behind this defective A–P growth defects, we carefully examined cellular proliferation in different regions of the PSs. We performed PHH3 immunofluorescence staining on E13.5 control and β-Catenin cKO PSs, and counted the number of PHH3 positive cells in a fixed region of anterior, middle and posterior palate. We found no difference in cell proliferation in any of the experimental groups (Fig. 4). These data suggested that loss of β-Catenin in the oral epithelium did not disturb normal cellular proliferation. The unique phenotype of retarded A–P growth but accelerated mediolateral growth suggested a disturbance in growth orientation rather than a lack of growth.

Since rugae form through sequential additions along the A–P axis, its formation may promote rostral outgrowth of the hard palate. Thus absence of rugae, and consequently rugae-specific morphogens, may disrupt the molecular guidance required to modulate growth orientation. To test this hypothesis, we examined the expression of two rugae-specific morphogen, *Shh* and *Bmp7*, in controls and mutants. Robust *Shh* expression can be detected in the incisors, primary palate and rugae epithelium throughout palatal development in controls (Fig. 5A–C). At e13.5, no Shh stripes were detected and only weak and sporadic

Shh expression remained in the secondary palate (Fig. 5D), which was consistent with the incomplete removal of β-Catenin at this stage (Fig. 1N and Supplemental Fig. S6). The expression in incisors was not detectable, and the expression domain in the primary palate region was reduced. From E14.5 onward, *Shh* expression was undetectable in the mutant palates (Fig. 5E, F). *Ptch1* expression was also downregulated at E13.5, consistent with a reduction in Hh signaling (Fig. 5H).

Bmp7 is also a rugae-specific morphogen, and it's speculated that Bmp7 might function as a negative regulator in the reaction-diffusion model to inhibit new rugae formation around existing rugae (Pantalacci et al., 2008). In controls, *Bmp7* was detected in the palatal rugae as well as the medial edge in controls from e13.5 to e15.5(Fig. 5I–K). In the mutants, its rugae expression was undetectable, but the medial edge expression was largely maintained (Fig. 5L–N).

These data indicated that the periodic morphogen gradient along A–P axis was not established in the mutant. Since Shh plays a key role in A–P patterning and expansion of the limb bud, we hypothesized that lack of Shh guidance caused A–P truncation of the hard palate. To examine the function of Shh in this process, we used a conditional knockout approach where we employed a conditional knockout *Shh* allele (Lewis et al., 2001) in combination with a Tamoxifen (Tm)-inducible Cre allele knocked into *Shh* locus (Harfe et al., 2004) (also resulted in a null allele). We treated pregnant mother at 10.5 day post-coitus to allow complete recombination and examined palatal development at E14.5. Indeed, the palatal phenotypes of Shh cKOs (Fig. 5P) remarkably resembled those of β-Catenin cKOs (Fig. 5P inset). Shh-cKO also showed lack of rugae formation, slightly reduced A–P expansion, and a poorly formed primary-secondary palatal junction. These Shh-cKO animals also developed complete cleft secondary palate which prevented us from assessing fusion between primary and secondary palate. The cleft palate phenotype in the Shh-cKO animals were consistent with several previous studies (Lan and Jiang, 2009; Rice et al., 2004). Altogether, these data suggested that the continuous addition of palatal rugae and consequently the establishment of periodic Shh gradient are critical for A–P extension of the secondary palates.

Finally, we didn't detect any PS fusion defect in the β-Catenin-cKOs (Supplemental Fig. S7B–C) other than the precocious fusion (Fig. 2C–F). However, we detected residual β-Catenin protein in the MEE of the mutant palates before fusion starts (Supplemental Fig. S7A). Thus, a role for Wnt in mediating palatal fusion cannot be addressed by our model.

Canonical Wnt responsiveness in the oral epithelium is essential for tongue formation

In addition to palatal abnormalities, we also uncovered defective tongue formation in β-Catenin cKO mutants resulted from loss of β-Catenin in the lingual epithelium (Fig. 6A–D). In controls, tongue development commences at around E11.5, when two lateral tongue swellings emerge from the floor of the mandibular processes. As development progresses, a third swelling, termed tuberculum impar, develops at the position of the second branchial arch. They eventually join together to form a single tongue at around E12.0–12.5. At E14.5 taste papillae, distinct structures on the tongue epithelium, can be readily detected (Fig. 6E, G, and I). Mutant tongue exhibited retarded growth from the very beginning. The two lateral swellings of the primitive tongue in mutants were smaller at E11.5 (Fig. 6F). At E12.5 when two lingual swellings met at the midline in controls, they remained separated in mutants. In addition, merging between tuberculum impar and two lingual swellings was also defective (Fig. 6H). At E14.5, the mutant tongue was much smaller, deformed and completely lacked taste papillae (Fig. 6J). The tongue is largely composed of CNC-derived mesenchyme and mesodermally-derived muscles. To evaluate the cellular basis of the mutant tongue defect, we examined the expression of Myf5, a marker for myogenic cell lineage. We found a

comparable number of Myf5-expressing cells in the mandibular region of both controls and mutants. However, Myf5-negative CNC cells were depleted in the mutants (indicated by double-headed arrows in Fig. 6K, L). Whereas H&E analysis on E13.5 control tongues revealed a loosely packed mesenchymal layer in-between epithelium and skeletal muscle, this cell population was reduced, disorganized and more compacted in the mutant (indicated by double-headed arrows in Fig. 6M, N). These data indicate that defective CNC development is likely the underlying mechanism for the mutant phenotype. Shh signaling is known to regulate CNC cell survival and proliferation (Jeong et al., 2004), and has been implicated in tongue development (Liu et al., 2004). Given our finding that *Shh* expression in the rugae requires Wnt activation, we reasoned that a similar regulatory circuitry may also occur in tongue development. We therefore examined gene expression of the Shh pathway in E11.5 control and mutant embryos. We found a striking downregulation of *Shh* expression in the mutant tongue epithelium (Fig. 7B). Consistently, *Ptch1* expression was also downregulated in mutant epithelium as well as in the underlying mesenchyme (Fig. 7D). The expression of *Gli1*, a downstream mediator of Shh signaling, was also reduced in the mutant (Fig. 7F). On the contrary, expression of *Fgf8* and *Wnt5a*, two other molecules critical for organ outgrowth, was preserved in the mutant tongue (Fig. 7G–J). Altogether, these results indicated that loss of Wnt signaling in the oral epithelium caused specific reduction of Shh signaling activity probably through downregulation of *Shh* ligand expression.

To probe into the consequence of reduced Shh signaling during tongue development, we adopted the same inducible *Shh* cKO model as described above. We gave pregnant females Tm at 10.5 days post-coitus (d.p.c.) to allow inactivation of *Shh* gene right at the stage of tongue initiation. We found an underdevelopment of *Shh* cKO mutant tongue at E12.5, confirming that lack of Shh signaling was sufficient to cause defective tongue formation in vivo (Fig. 7L). Altogether, we demonstrated that activation of *Shh* expression by canonical Wnt-β-Catenin signaling pathway in lingual epithelium is a crucial event for early tongue development.

DISCUSSION

In this study, we used tissue-specific knock-out mouse to investigate the role of Wnt responsiveness in the oral epithelium. We demonstrated that Wnt-β-Catenin pathway in both palatal rugae and tongue epithelium plays dynamic roles in craniofacial development.

The initial development of a variety of ectodermal appendages, including that of palatal rugae, shares remarkable similarities involving thickening of the epithelium (formation of placode) and condensation of the underlying mesenchyme. The genetic cassette required for patterning epithelial appendages is also likely to be conserved. From feathers in birds(Noramly et al., 1999), hair follicles (Andl et al., 2002; Huelsken et al., 2001), taste buds (Liu et al., 2007), teeth (Liu et al., 2008a) and mammary glands (Chu et al., 2004) in mammals to ostia in sponges (Lapebie et al., 2009), the early induction of placodes requires deployment of canonical Wnt pathway. In this study, we established that activation of Wnt signaling was absolutely essential in palatal rugae development. The fact that epithelial placode and mesenchymal condensation failed to form, as well as the lack of any known rugae marker expression in the β-Catenin cKO palate indicated that Wnt signaling is obligatory in rugae initiation. This function is reminiscent of its role in the development of other ectodermal appendages, such as hair and tooth. However, the exact mechanism whereby Wnt activity is initiated during induction of all these aforementioned appendages remains obscure. In most cases, complete abolishment of appendage formation as a result of either β-Catenin cKOs or inhibitor overexpression has not been fully recapitulated by knocking out one or more Wnt ligands. Genetic redundancy among Wnt ligands is an

obvious speculation, whereas additional regulatory mechanisms might also be involved. Indeed, elevated mRNA expression of *β-Catenin* was noted at perspective appendage sites both in our study on rugae formation and in previous studies on hair follicle and mammary gland development. These data suggest that regulation of *β-Catenin* transcription, in addition to Wnt signaling-mediated protein stabilization, also contributes to signal initiation/propagation. Moreover, the fact that Wnt activity reporter can be detected even earlier than localized ligand expression (Chu et al., 2004) suggests that factors outside of the Wnt family might also be involved in establishing and modulating the initial Wnt responsiveness.

It is also noteworthy that all but one rugae are formed at the same position relative to the most posterior ruga, which indicates that the initiation and/or inhibition signals likely have differential expression in that region. This expression could result from interactions between cells from the hard and soft palates as the position of the last rugae also correlates with the boundary between hard and soft palates. However, we did not detect any Wnt family genes, either ligands or inhibitors, that exhibit differential expression in that particular domain, suggesting the involvement of other regulatory elements during placode induction. One such candidate is Fgf10 (Welsh and O'Brien, 2009), which has a patterned expression around the rugae forming region. The mesenchymal expression of *Fgf10* was shown to be an event upstream of induction of the epithelial signaling center in limb development (Sekine et al., 1999). Future analysis on interactions between Fgf10 and WNT signaling pathway may help us understand the process of rugae initiation.

The stereotypic interposition of palatal rugae also suggests a reaction-diffusion mechanism (Turing, 1952) that is widely proposed to explain the spacing of skin appendages. However, such a mechanism has to be carefully interpreted within the context of palatal expansion. We demonstrated that the rugaeless β-Catenin cKO palate has a retarded A–P growth of *Shox2*-expressing anterior palate and an accelerated lateral expansion, a unique phenotype that has not been observed in any other mutants. This phenotype suggests that addition of rugae might serve as a mechanism for the hard palate to balance anteroposterior and mediolateral growth, which is achieved through periodically acquiring morphogen cues required for guiding rostral outgrowth. A–P extension of the hard palate is necessary for creating a disequilibrium projected by reaction-diffusion model that permits the induction of the next appendage. And in turn, the newly formed ruga will provide additional morphogens or chemoattractants, e.g. Shh, to ensure that palate extends further along (Fig. 5Q). One also has to keep in mind that the development of the oral structures is likely coordinated. We cannot exclude the possibility that the overgrowth of the PSs along the medial-lateral edge might be secondary to the lack of tongue development in both β-Catenin and Shh cKOs. However, there is no direct evidence supporting that abnormal tongue development affects the A–P patterning and growth of the secondary palate. We also liked to emphasize that in our current model, β-Catenin deletion is not rugae-specific but rather extends to the entire ventral palatal epithelium. Therefore, mechanisms other than rugae deficiency may also contribute to the phenotype. We attempted to address this issue by restricting Cre activity only in rugae epithelium using an inducible Shh^{Creesr} line (Harfe et al., 2004). However, this approach failed to achieve β-Catenin deletion even after three consecutive Tamoxifen treatments (oral gavage) at a concentration of 0.2g/kg body weight (from e11.5-e13.5) evidenced by immunofluorescence analysis (Supplemental Fig. S8). This is likely due to the low accessibility of the β-Catenin genomic locus in palatal epithelium, as one shot of Tamoxifen at the same concentration can achieve complete deletion in urethral epithelium (Lin et al., 2008).

Notably, a recent study (He et al., 2011) using the K14-Cre transgene to target β-Catenin showed a complete cleft secondary palate with high penetrance and a role for Wnt signaling in mediating apoptosis of the MEE is proposed. However, in this mutant model A–P

development of the secondary palate, tongue development and primary palate development were not described (He et al., 2011). The phenotypic differences between the two models likely reflect subtle variations in the temporal and spatial expression pattern of the Cre transgene. Shh-Cre used in this study mediates gene deletion in the ventral epithelium but not in the MEE, where K14-Cre is apparently more effective evidenced by the high penetrance of complete cleft secondary palate. Shh-Cre expression can be detected at around e11.5 throughout the oral epithelium. However, complete deletion of β-Catenin is not achieved in the ventral palatal epithelium until e14.5. The temporal and spatial expression of the K14-Cre and the timing of the actual protein ablation was not clear, although RNA in situ analysis showed a marked downregulation of β-Catenin transcripts at e13.5 (He et al., 2011). It's important to note that findings in these two models are not contradictory but rather reflect different roles for β-Catenin in oral development.

The mechanism underlying the cleft palate phenotype in our Shh-Cre model is likely the underdevelopment of the primary palate but not the fusion defect as observed in the K14-Cre model, as revealed by both SEM analysis and histological analysis on e15.5 (Fig. 2). The defective rostral outgrowth of the hard palates may also contribute to the cleft palate phenotype observed in our model.

Our analysis also revealed a novel role for Wnt signaling in the lingual epithelium to induce *Shh* expression and regulate early development of the tongue primordia. This regulation appeared to be particularly important for CNC-derived fibroblasts, which might signal to and provide structural support for myogenic differentiation. These findings reiterate that interactions between oral-epithelium and CNC-derived mesenchyme is a critical step for tongue formation. Unfortunately, the exact mechanism through which β-Catenin regulates Shh expression is still not clear.

Supplementary Material

Refer to Web version on PubMed Central for supplementary material.

Acknowledgments

We thank Dr. Yiping Chen for exchanging progress before submission. We thank Jaclynn Lett, and Washington University in St. Louis, Department of Otolaryngology, Research Center for Auditory and Visual Studies (funded by NIH P30 DC004665) for providing technical assistance on Electron Microscopy. This work is funded by NIH grants ES014482 and ES01659701 (L. M.) and American Urological Association research scholar program (C. L.).

References

Andl T, Reddy ST, Gaddapara T, Millar SE. WNT signals are required for the initiation of hair follicle development. Dev Cell. 2002; 2:643–53. [PubMed: 12015971]

Barrow JR, Thomas KR, Boussadia-Zahui O, Moore R, Kemler R, Capecchi MR, McMahon AP. Ectodermal Wnt3/beta-catenin signaling is required for the establishment and maintenance of the apical ectodermal ridge. Genes Dev. 2003; 17:394–409. [PubMed: 12569130]

Brault V, Moore R, Kutsch S, Ishibashi M, Rowitch DH, McMahon AP, Sommer L, Boussadia O, Kemler R. Inactivation of the beta-catenin gene by Wnt1-Cre-mediated deletion results in dramatic brain malformation and failure of craniofacial development. Development. 2001; 128:1253–64. [PubMed: 11262227]

Brugmann SA, Goodnough LH, Gregorieff A, Leucht P, ten Berge D, Fuerer C, Clevers H, Nusse R, Helms JA. Wnt signaling mediates regional specification in the vertebrate face. Development. 2007; 134:3283–95. [PubMed: 17699607]

Chu EY, Hens J, Andl T, Kairo A, Yamaguchi TP, Brisken C, Glick A, Wysolmerski JJ, Millar SE. Canonical WNT signaling promotes mammary placode development and is essential for initiation of mammary gland morphogenesis. Development. 2004; 131:4819–29. [PubMed: 15342465]

DasGupta R, Fuchs E. Multiple roles for activated LEF/TCF transcription complexes during hair follicle development and differentiation. Development. 1999; 126:4557–68. [PubMed: 10498690]

Gorlin, RJCMJ.; Hennekam, RCM. Syndromes of the head and neck. New York: Oxford University Press; 2001.

Gritli-Linde A. Molecular control of secondary palate development. Dev Biol. 2007; 301:309–26. [PubMed: 16942766]

Harfe BD, Scherz PJ, Nissim S, Tian H, McMahon AP, Tabin CJ. Evidence for an expansion-based temporal Shh gradient in specifying vertebrate digit identities. Cell. 2004; 118:517–28. [PubMed: 15315763]

He F, Xiong W, Wang Y, Li L, Liu C, Yamagami T, Taketo MM, Zhou C, Chen Y. Epithelial Wnt/beta-catenin signaling regulates palatal shelf fusion through regulation of Tgfbeta3 expression. Dev Biol. 2011; 350:511–9. [PubMed: 21185284]

Hosokawa R, Oka K, Yamaza T, Iwata J, Urata M, Xu X, Bringas P Jr, Nonaka K, Chai Y. TGF-beta mediated FGF10 signaling in cranial neural crest cells controls development of myogenic progenitor cells through tissue-tissue interactions during tongue morphogenesis. Dev Biol. 2010; 341:186–95. [PubMed: 20193675]

Huelsken J, Vogel R, Erdmann B, Cotsarelis G, Birchmeier W. beta-Catenin controls hair follicle morphogenesis and stem cell differentiation in the skin. Cell. 2001; 105:533–45. [PubMed: 11371349]

Jeong J, Mao J, Tenzen T, Kottmann AH, McMahon AP. Hedgehog signaling in the neural crest cells regulates the patterning and growth of facial primordia. Genes Dev. 2004; 18:937–51. [PubMed: 15107405]

Lan Y, Jiang R. Sonic hedgehog signaling regulates reciprocal epithelial-mesenchymal interactions controlling palatal outgrowth. Development. 2009; 136:1387–96. [PubMed: 19304890]

Lapebie P, Gazave E, Ereskovsky A, Derelle R, Bezac C, Renard E, Houliston E, Borchiellini C. WNT/beta-catenin signalling and epithelial patterning in the homoscleromorph sponge Oscarella. PLoS One. 2009; 4:e5823. [PubMed: 19503791]

Lewis PM, Dunn MP, McMahon JA, Logan M, Martin JF, St-Jacques B, McMahon AP. Cholesterol modification of sonic hedgehog is required for long-range signaling activity and effective modulation of signaling by Ptc1. Cell. 2001; 105:599–612. [PubMed: 11389830]

Li Q, Ding J. Gene expression analysis reveals that formation of the mouse anterior secondary palate involves recruitment of cells from the posterior side. Int J Dev Biol. 2007; 51:167–72. [PubMed: 17294368]

Lin C, Yin Y, Long F, Ma L. Tissue-specific requirements of beta-catenin in external genitalia development. Development. 2008; 135:2815–25. [PubMed: 18635608]

Liu F, Chu EY, Watt B, Zhang Y, Gallant NM, Andl T, Yang SH, Lu MM, Piccolo S, Schmidt-Ullrich R, et al. Wnt/beta-catenin signaling directs multiple stages of tooth morphogenesis. Dev Biol. 2008a; 313:210–24. [PubMed: 18022614]

Liu F, Thirumangalathu S, Gallant NM, Yang SH, Stoick-Cooper CL, Reddy ST, Andl T, Taketo MM, Dlugosz AA, Moon RT, et al. Wnt-beta-catenin signaling initiates taste papilla development. Nat Genet. 2007; 39:106–12. [PubMed: 17128274]

Liu HX, Maccallum DK, Edwards C, Gaffield W, Mistretta CM. Sonic hedgehog exerts distinct, stage-specific effects on tongue and taste papilla development. Dev Biol. 2004; 276:280–300. [PubMed: 15581865]

Liu W, Lan Y, Pauws E, Meester-Smoor MA, Stanier P, Zwarthoff EC, Jiang R. The Mn1 transcription factor acts upstream of Tbx22 and preferentially regulates posterior palate growth in mice. Development. 2008b; 135:3959–68. [PubMed: 18948418]

Maretto S, Cordenonsi M, Dupont S, Braghetta P, Broccoli V, Hassan AB, Volpin D, Bressan GM, Piccolo S. Mapping Wnt/beta-catenin signaling during mouse development and in colorectal tumors. Proc Natl Acad Sci U S A. 2003; 100:3299–304. [PubMed: 12626757]

Niemann S, Zhao C, Pascu F, Stahl U, Aulepp U, Niswander L, Weber JL, Muller U. Homozygous WNT3 mutation causes tetra-amelia in a large consanguineous family. Am J Hum Genet. 2004; 74:558–63. [PubMed: 14872406]

Noramly S, Freeman A, Morgan BA. beta-catenin signaling can initiate feather bud development. Development. 1999; 126:3509–21. [PubMed: 10409498]

Nunzi MG, Pisarek A, Mugnaini E. Merkel cells, corpuscular nerve endings and free nerve endings in the mouse palatine mucosa express three subtypes of vesicular glutamate transporters. J Neurocytol. 2004; 33:359–76. [PubMed: 15475690]

Pantalacci S, Prochazka J, Martin A, Rothova M, Lambert A, Bernard L, Charles C, Viriot L, Peterkova R, Laudet V. Patterning of palatal rugae through sequential addition reveals an anterior/posterior boundary in palatal development. BMC Dev Biol. 2008; 8:116. [PubMed: 19087265]

Rice R, Spencer-Dene B, Connor EC, Gritli-Linde A, McMahon AP, Dickson C, Thesleff I, Rice DP. Disruption of Fgf10/Fgfr2b-coordinated epithelial-mesenchymal interactions causes cleft palate. J Clin Invest. 2004; 113:1692–700. [PubMed: 15199404]

Sekine K, Ohuchi H, Fujiwara M, Yamasaki M, Yoshizawa T, Sato T, Yagishita N, Matsui D, Koga Y, Itoh N, et al. Fgf10 is essential for limb and lung formation. Nat Genet. 1999; 21:138–41. [PubMed: 9916808]

Soshnikova N, Zechner D, Huelsken J, Mishina Y, Behringer RR, Taketo MM, Crenshaw EB 3rd, Birchmeier W. Genetic interaction between Wnt/beta-catenin and BMP receptor signaling during formation of the AER and the dorsal-ventral axis in the limb. Genes Dev. 2003; 17:1963–8. [PubMed: 12923052]

Turing, AM. Philosophical Transactions of the Royal Society of London. 1952. The chemical basis of morphogenesis.

Wawersik S, Epstein JA. Gene expression analysis by in situ hybridization. Radioactive probes. Methods Mol Biol. 2000; 137:87–96. [PubMed: 10948528]

Welsh IC, O'Brien TP. Signaling integration in the rugae growth zone directs sequential SHH signaling center formation during the rostral outgrowth of the palate. Dev Biol. 2009; 336:53–67. [PubMed: 19782673]

Widera D, Zander C, Heidbreder M, Kasperek Y, Noll T, Seitz O, Saldamli B, Sudhoff H, Sader R, Kaltschmidt C, et al. Adult palatum as a novel source of neural crest-related stem cells. Stem Cells. 2009; 27:1899–910. [PubMed: 19544446]

Wilkinson, D. In Situ Hybridization; a Practical Approach. London: Oxford University Press; 1992.

Yin Y, Lin C, Ma L. MSX2 promotes vaginal epithelial differentiation and wolffian duct regression and dampens the vaginal response to diethylstilbestrol. Mol Endocrinol. 2006; 20:1535–46. [PubMed: 16513791]

Yu HM, Jerchow B, Sheu TJ, Liu B, Costantini F, Puzas JE, Birchmeier W, Hsu W. The role of Axin2 in calvarial morphogenesis and craniosynostosis. Development. 2005a; 132:1995–2005. [PubMed: 15790973]

Yu L, Gu S, Alappat S, Song Y, Yan M, Zhang X, Zhang G, Jiang Y, Zhang Z, Zhang Y, et al. Shox2-deficient mice exhibit a rare type of incomplete clefting of the secondary palate. Development. 2005b; 132:4397–406. [PubMed: 16141225]

Zhang Z, Song Y, Zhao X, Zhang X, Fermin C, Chen Y. Rescue of cleft palate in Msx1-deficient mice by transgenic Bmp4 reveals a network of BMP and Shh signaling in the regulation of mammalian palatogenesis. Development. 2002; 129:4135–46. [PubMed: 12163415]

Highlights

- We report that conditional knockout of β-Catenin, the obligatory mediator of canonical Wnt signaling, in the oral epithelium caused pleiotropic defects in the development of oral structures.
- Abolishing Wnt responsiveness completely blocks the formation of palatal rugae, which are specialized ectodermal appendages serving as Shh signaling centers
- >Lack of rugae in the mutant is also associated with retarded antero-posterior extension of the secondary palate and precocious midline fusion. >We also show that β-Catenin cKO tongues are severely underdeveloped.

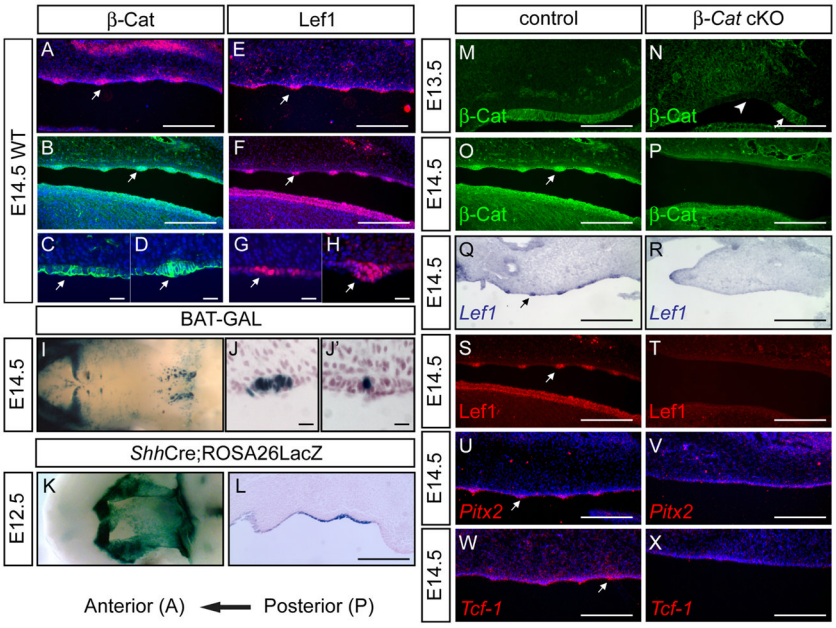

Fig. 1.

Activation of Wnt signaling in the palatal rugae. (A, E) In situ hybridization using *β-Catenin* (A) and *Lef-1* (E) probes on WT E14.5 sagittal sections. (B–D, F–H) Immunostaining on E14.5 palates using β-Catenin (B–D) or Lef1 (F–H) antibodies. Note elevated expression in the most developed boundary ruga (arrows in D and H), and in the newly forming ruga anterior to it (arrows in C and G). (I) Whole mount stained e14.5 BATGAL palate showing strong anterior rugae staining and weak posterior rugae staining. (J, J′) Sagittal sections of whole mount stained e14.5 BATGAL palate showing positive staining in both anterior ruga (J) and posterior ruga (J′). (K, L) X-gal staining of E12.5 $Shh^{cregfp/+}$; R26R palate showing palatal epithelial staining. (M–P) β-Catenin immunostaining showing residual β-Catenin in E13.5 β-Catenin cKO palate (arrow in N) but complete loss of β-Catenin at E14.5 (P). (Q–T) *Lef1* in situ (Q, R) and immunostaining (S, T) on E14.5 palatal sections showing loss of rugae expression in β-Catenin cKO. (U, V) *Pitx2* and (W, X)*Tcf1* in situ on E14.5 control and β-Catenin cKO palates. Scale bars in A, B, E, F, L, O-X and L: 0.25mm; in M and N: 0.12mm; in C, D, G and H:20μm; in J and J′:10μm

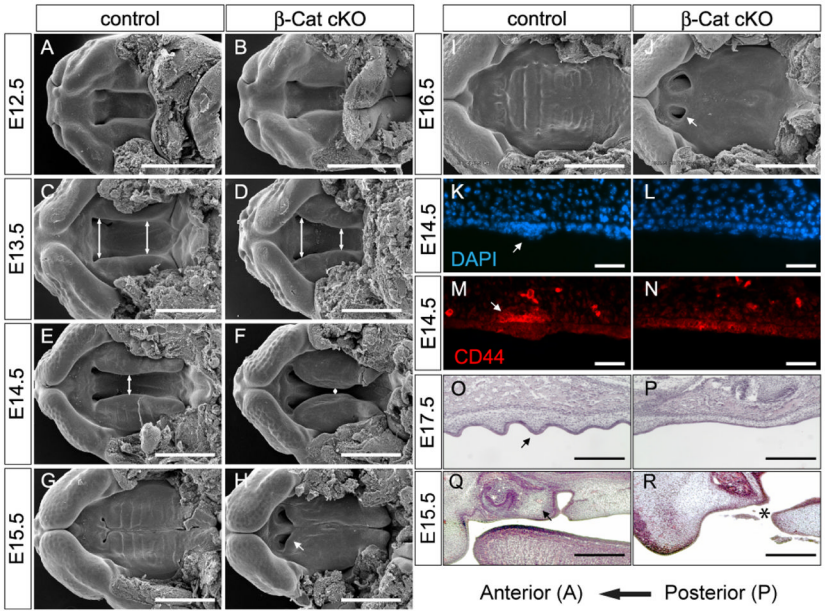

Fig. 2.

Phenotype of β-Catenin cKO palates. (A–J) SEM on β-Catenin cKO and control palates. The distance between two PSs was indicated by double-headed arrows. (K, L) DAPI staining showing lack of placode formation in β-Catenin cKOs. (M, N) CD44 staining showing no mesenchymal condensation in β-Catenin cKO palates. (O, P) H&E staining showing developed rugae in control and lack of rugae in β-Catenin cKO at E17.5. (Q, R) H&E staining showing that the primary palate (arrow in Q) meets with the secondary palate in the e15.5 control embryos, whereas in the mutant, the primary palate was underdeveloped and did not meet with the secondary palate (asterisk in R). Scale bars in A–J: 1mm; in K–N: 30μm; in O–R: 0.25mm.

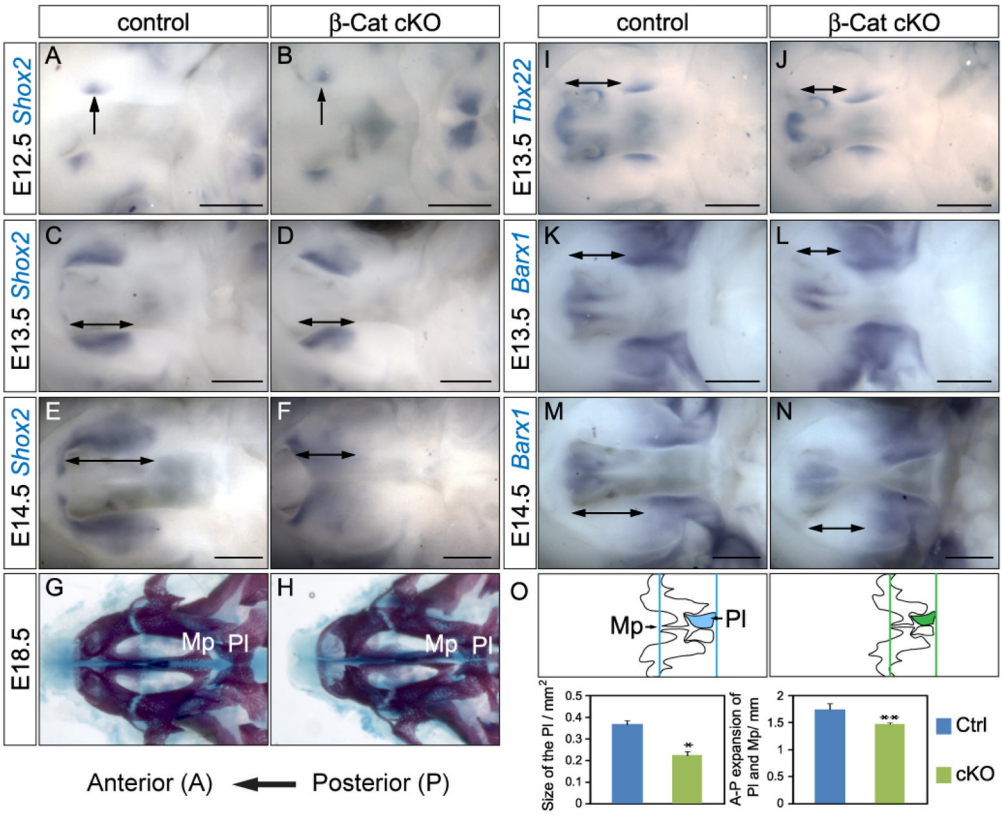

Fig. 3.

Hard palate defect in β-Catenin cKOs. (A–F) *Shox2* in situ at stages indicated. Note comparable *Shox2* expression in E12.5 (B), altered expression domain in E13.5 (D) and reduced expression in E14.5 (F). (I, J) *Tbx22* in situ showing comparable posterior expression in both genotypes. (K–N) *Barx1* in situ showing comparable expression in the cKO, note that the *Barx1*-negative region in the cKOs (L, N) is smaller than the controls (K, M). The A–P expansion of the hard palate was indicated by double-headed arrows in C–F and I–N. (G–H, and O) Skeletal preparation of E17.5 embryonic heads showing a smaller palatine bone (Pl, highlighted in O) and reduced A–P expansion of palatine bone and maxillary processes (Mp) (distance between two colored vertical lines in the scaled schematic representations) in the mutant (n=4 for each experiment, $p<0.001$ for the size of Pl, $p=0.014$ for A–P expansion of Pl and Mp). Scale bars: 0.5mm.

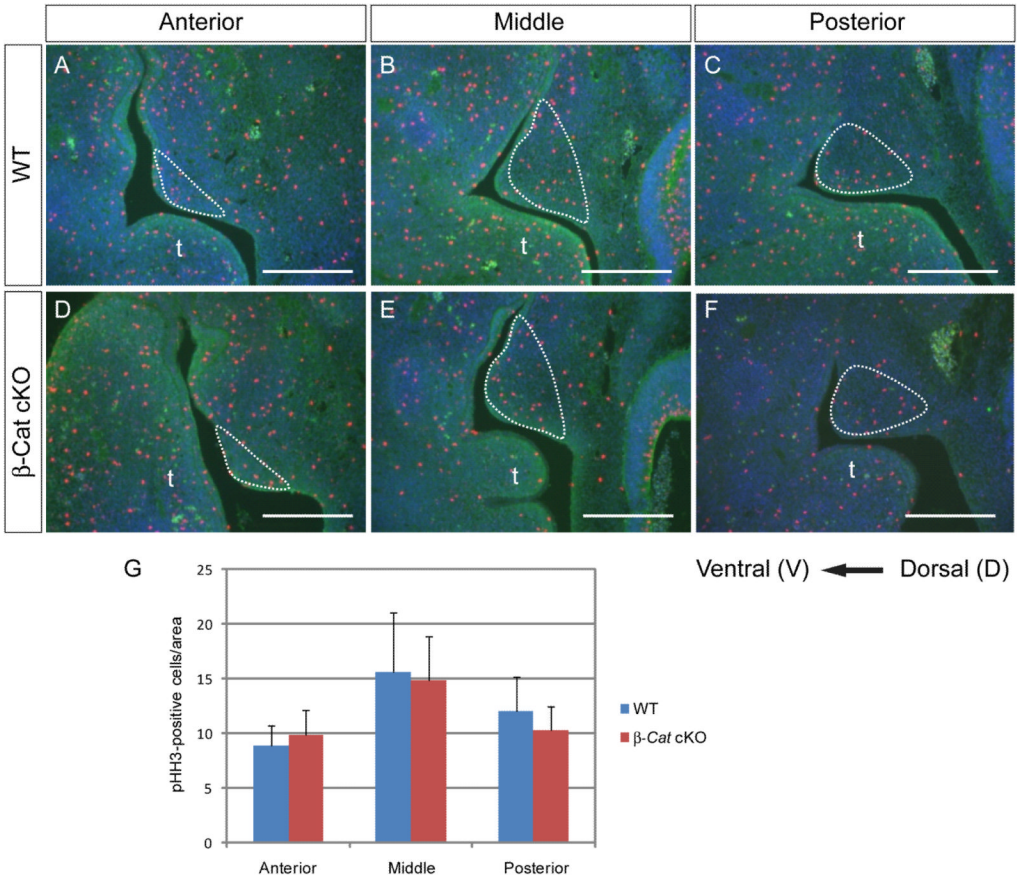

Fig. 4.

Cell proliferation in control and β-Catenin cKO palatal shelves. (A–F) PHH3 staining on anterior (A, D), middle (B, E) and posterior (C, F) palatal shelves of WT (A–C) and β-Catenin-cKO palates (D–F) showed no difference in proliferation rate (n=8) (G). The palatal region was highlighted and the position of tongue (t) was indicated in the figure. Scale bars: 0.25mm

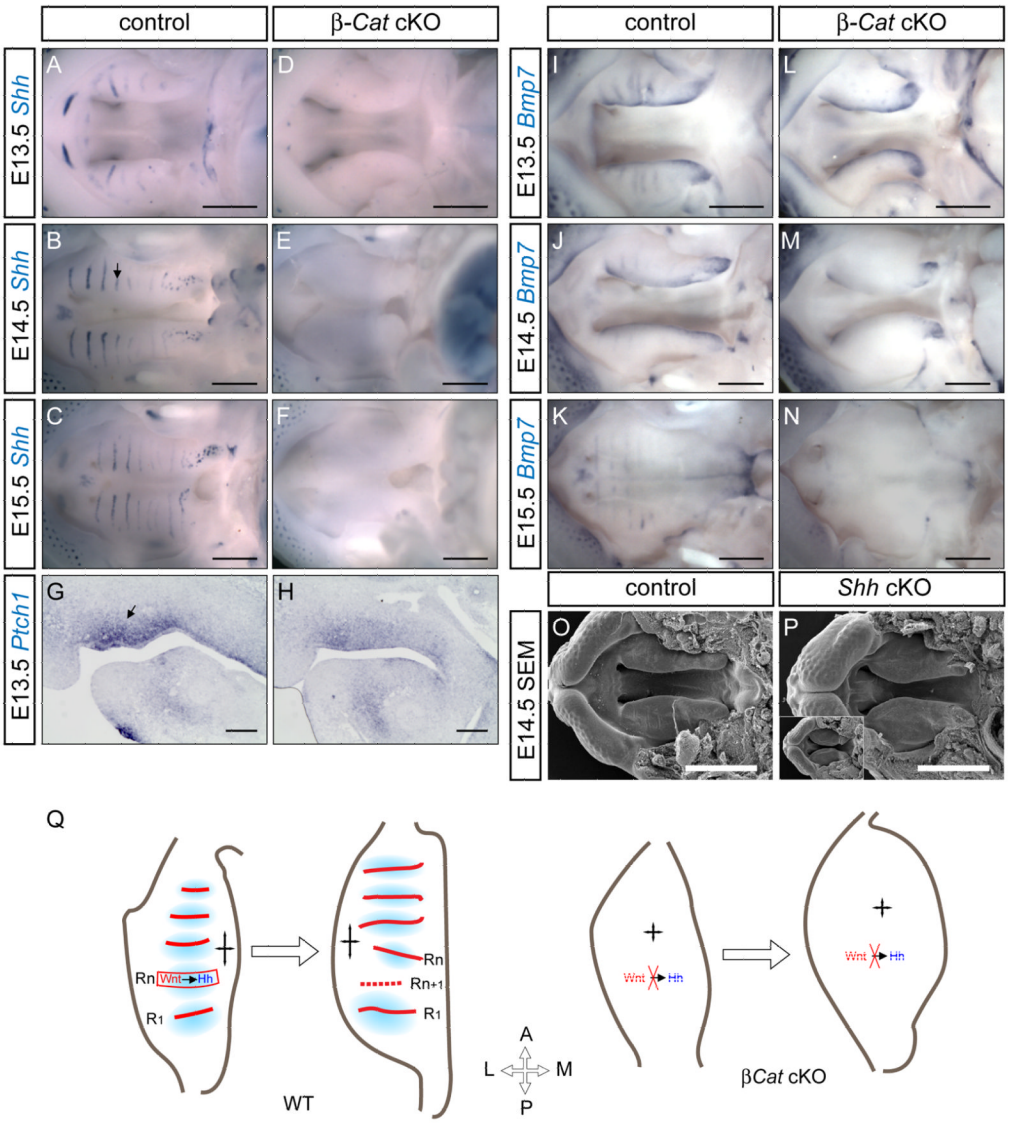

Fig. 5.

Lack of rugae specific-morphogen expression in β-Catenin cKO. (A–F) *Shh* in situ at stages indicated. (G, H) *Ptch1* in situ on E13.5 control and β-Catenin cKO sections. (I–N) *Bmp7* in situ at stages indicated. (O, P) SEM on E14.5 control and *Shh* cKO palates (P). β-Catenin cKO palate at the same stage was presented as an inset in (P) for comparison. (Q) In WT palate, active Wnt signaling (red) in rugae establishes a Shh gradient (blue), which guides palatal growth along the A–P axis (quad arrow). As palate elongates and the distance between R1 and Rn increases, ruga Rn_{+1} emerges in-between them (dashed line). In β-Catenin cKO, absence of Wnt and subsequent Shh morphogen expression results in unregulated tissue expansion, leading to undergrowth anteroposteriorly and overgrowth mediolaterally. Scale bars: A–F and I–N: 0.5mm; in G and H: 0.25mm; in O and P: 1mm.

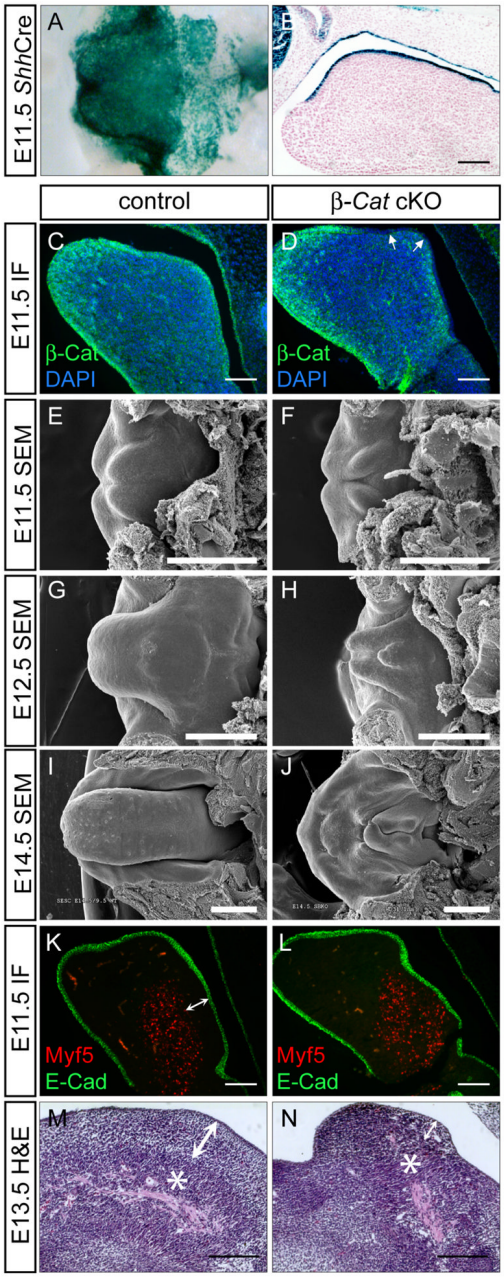

Fig. 6.

Microglossia in β-Catenin cKO embryos. X-gal staining on whole mount (A) or sagittal section (B) of E11.5 *Shh*$^{cregfp/+}$; R26R embryo showing tongue epithelial expression. (C, D) β-Catenin Immunostaining on E11.5 control and cKO showing complete removal of the protein from the dorsal tongue epithelium (arrows in D). (E–J) SEM analysis on E11.5–E14.5 control and mutant tongues. (K, L) Double immunofluorescence analysis using antibodies against E-Cadherin (green) and Myf-5 (red) showing comparable Myf-5 positive cell population, and a lack of Myf-5 negative cells (indicated by double-headed arrows) in the cKO. (M, N) H&E staining on E13.5 sagittal sections showing a loosely-packed mesenchyme in control (double-headed arrow in M, muscles was indicated by asterisks) and

disorganized and reduced mesenchyme in the cKO (double headed arrow in N, muscle was indicated by asterisk). Scale barsin E–H: 1mm, in I and J: 0.5mm; in B–D and K–N: 0.5mm

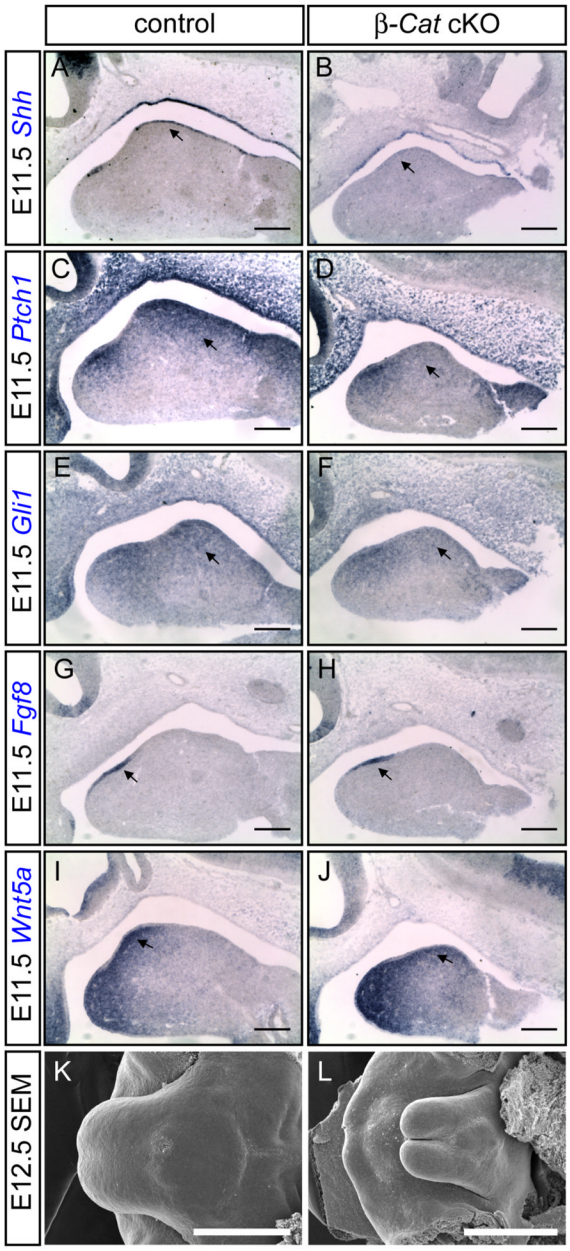

Fig. 7.

Reduced Shh signaling in β-Catenin cKO tongue. (A–J) In situ hybridization on E11.5 β-Catenin cKO and control tongues using probes indicated. Note the downregulation of *Shh* in the tongue epithelium, and *Ptch1* and *Gli1* in the mesenchyme. (K, L) SEM analysis on E12.5 control and Shh cKO tongue showing an underdeveloped tongue in the mutant (L). Scale bars in A–J: 0.5mm; in K and L: 1mm.